Malaysian Journal of Mathematical Sciences 17(3): 441–458 (2023)
https://doi.org/10.47836/mjms.17.3.12

Malaysian Journal of Mathematical Sciences

Journal homepage: https://mjms.upm.edu.my

Behaviour of the Onset of Rayleigh-Bénard Convection in Double-Diffusive Micropolar Fluids Under the Influence of Cubic Temperature and Concentration Gradient

Idris, R.*[1], Alias, A.[1], and Miqdady, A.[1]

[1]*Special Interest Group for Modelling and Data Analytics, Faculty of Ocean Engineering Technology and Informatics, Universiti Malaysia Terengganu, 21030 Kuala Nerus, Terengganu, Malaysia*

E-mail: ruwaidiah@umt.edu.my
**Corresponding author*

Received: 22 June 2023
Accepted: 8 August 2023

Abstract

Convection heat transfer especially Rayleigh-Bénard convection plays a significant role either in nature or industry applications. Particularly, in industry, the instability of the Rayleigh-Bénard convection process is important to see whether the quality of final goods is excellent or not. Therefore, in this study linear stability theory has been performed to investigate the influence of cubic temperature gradient and cubic concentration gradient on the onset of convection in a double-diffusive micropolar fluid. By adopting the single-term Galerkin procedure, parameters N_1, N_3, N_5, and Rs have been analyzed to investigate their influence on the onset of convection. The results found that the coupling parameter N_1 and micropolar heat conduction parameter N_5 will put the system in stable conditions. Meanwhile, the couple stress parameter N_3 and solutal Rayleigh number Rs will destabilize the system. The results also show that by increasing the value of the solutal Rayleigh number Rs, the value of the critical Rayleigh number Ra_c will decrease. By enclosing the micron-sized suspended particles, we can slow down the process of Rayleigh-Bénard convection in double-diffusive micropolar fluids. It is possible to control the process of the onset of Rayleigh-Bénard convection by selecting suitable non-uniform temperature and concentration gradient profiles.

Keywords: Rayleigh-Bénard convection; temperature gradient; concentration gradient; micropolar fluids; double-diffusive; single-term Galerkin technique.

1 Introduction

The study of the dynamic behavior of the physical system in natural and industrial applications has been made in understanding the idea of convection in fluid over the past century and continues to be a growth of interest in mathematical inspiration. Convection is the process that combines advection and diffusion to move the cluster of molecules within fluids in a coordinated manner. The difference in temperature leads to density variation in fluids which gives rise to natural convection where the convective motions produced by unstable density distributions in a fluid such as in a thin horizontal layer of fluid, heated at the bottom and cooled at the upper surface have been successfully studied theoretically and experimentally [3]. This phenomenon is also known as Rayleigh-Bénard convection and Bénard-Marangoni convection.

In oceanography, warmth diffuses around 100 times more quickly than salt, thus the interaction of two separate density gradients (such as temperature and salinity) with varying rates of diffusion results in double-diffusive convection, which is important in the fluid dynamics phenomenon. Double diffuse effects were firstly observed by [21] and explained the physical mechanism responsible. Previous research discovered instability at the boundary between temperature-stratified water and a denser fluid layer, but only a few researchers had yet understood the importance of double-diffusion. [22] demonstrated that when a tube is introduced vertically through the junction between a layer of heated, salty water on top of a cool layer of fresh water, a *perpetual salt fountain* be forming. The fountain continues to flow until the system is thoroughly combined. *salt fingers* and *diffusive convection* are two examples of double-diffusive instability. [19].

[15] and [16] have considered the case when the base fluid of the nanofluid itself is a binary fluid such as salt water in a horizontal layer of a porous medium saturated with the nanofluid. They have discussed how the theory of double diffusion affects the initiation of convection in the nanofluid. Using the Galerkin method, the stability boundaries for both non-oscillatory and oscillatory modes were estimated assuming that the nanofluids model combines the effects of Brownian motion and thermophoresis and the Darcy model for porous media.

Meanwhile, [1] provided a summary of the characteristics of double-diffusive convection in a layer of porous media saturated with nanofluid. The linear stability was investigated using the normal mode technique and the nonlinear analysis was studied using the minimum representation of the truncated Fourier series analysis involving two terms. The results show that for the linear analysis, the critical value of the Rayleigh number has been obtained, while the term Nusselt number has been given for the nonlinear analysis. In order to address the properties of fluids with suspended particles, [4, 5] developed the theory of micropolar fluids. Analysis of the various applications of micropolar fluid mechanics was provided by [2, 12] and [18].

[13] investigated the influence of an internal heat source on the initiation of Rayleigh-Bénard convection in order to develop a control strategy method for double-diffusive convection using a nanofluid layer. By concentrating on stationary convection, they demonstrated that internal heat generation causes a positive thermal efficiency while feedback control on the initial stage of double-diffusive convection causes a positive thermal resistance. Meanwhile, [9] examined the effect of internal heat generation in the presence of Soret and Dufour effects on the magnetoconvection on the double-diffusive nanofluids layer. Using the Galerkin approach, they obtained that the system becomes stable with the presence of the magnetic field while becoming unstable when internal heat generation appears.

Rayleigh-Bénard convection's response to feedback control and double-diffusive coefficients was examined by [10]. They found that by increasing the value of rotation, the system can be sta-

bilized by using feedback control, the Dufour parameter, and the solutal Rayleigh number. In the meantime, the system becomes unstable as the values of the Soret parameter, nanofluids Lewis number, nanoparticle concentration Rayleigh number, and modified diffusivity ratio rise. A layer of a micropolar fluid subjected to double-diffusive convection was studied in [17], and the authors pointed out the impact of a non-uniform basic concentration gradient on the convective motion of this fluid layer. Using linear stability theory they explained in depth the effects of various micropolar parameters on the onset of convection. However, temperature and density differences commonly have an impact on convection, causing density variations in the fluid motion and leading to differences in concentration gradients.

Therefore, the main purpose of this research is to observe the behavior of the onset convection in double-diffusive micropolar fluids when both cubic temperature gradient and concentration gradients were considered as a control mechanism for the onset of convection. Three different velocity boundary combinations, namely Free-Free (f-f), Rigid-Free (r-f), and Rigid-Rigid (r-r) boundaries, are used to analyze the various types of temperature and concentration profiles. This problem is an extension of a concept from [17] who only took into account the situation for non-uniform concentration gradient. Both gradient equations for temperature and concentration are given in the general form in order to analyze how these parameters affect the systems, as mentioned in the linear stability analysis Section 3 (refer to [8]). The influence of several parameters will also be investigated to see their effect on the stability of the system.

2 Mathematical Problem Formulation

The stability of an infinite horizontal layer of Boussinesq double-diffusive micropolar fluids of depth d as shown in Figure 1 is the subject of this research. The temperature difference and species concentration difference of the fluid between the upper and lower plate are represented by $\Delta\vartheta$ and ΔS.

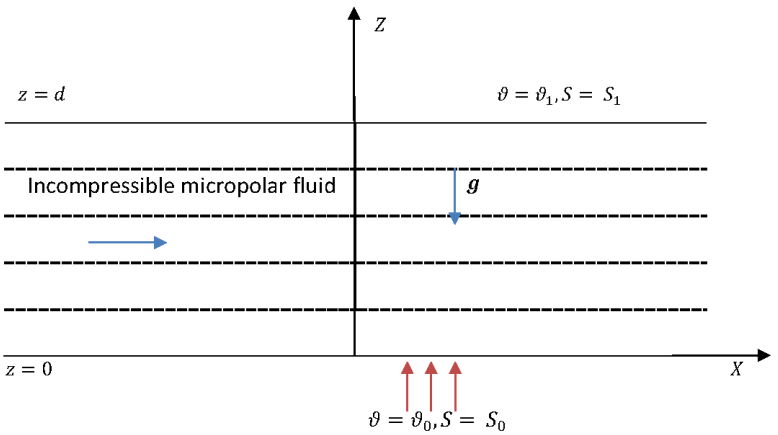

Figure 1: Model of schematic diagram.

The governing equations for the problem of double-diffusive micropolar fluids is given by the following equations (refer to: [17]):

Equation of Mass:

$$\nabla \cdot \mathbf{u} = 0. \tag{1}$$

Linear Momentum Equation:

$$\rho_0 \left[\frac{\partial \mathbf{u}}{\partial t} + (\mathbf{u} \cdot \nabla)\,\mathbf{u}\right] = -\nabla p - \rho \mathbf{g}\widehat{k} + (2\xi + \gamma)\,\nabla^2 \mathbf{u} + \xi \nabla \times \omega. \tag{2}$$

Angular Velocity Equation:

$$\rho_0 I \left[\frac{\partial \omega}{\partial t} + (\mathbf{u} \cdot \nabla)\,\omega\right] = (\lambda' + \gamma')\,\nabla\,(\nabla \cdot \omega) + \gamma' \nabla^2 \omega + \xi\,(\nabla \times \mathbf{u} - 2\omega)\,. \tag{3}$$

Energy Equation:

$$\left[\frac{\partial \vartheta}{\partial t} + (\mathbf{u} \cdot \nabla)\,\vartheta\right] = \chi \nabla^2 \vartheta + \frac{\beta}{\rho_0 C_v}\,(\nabla \times \omega) \cdot \nabla \vartheta. \tag{4}$$

Soluted Concentration Equation:

$$\left[\frac{\partial S}{\partial t} + (\mathbf{u} \cdot \nabla)\,S\right] = \chi_s \nabla^2 S. \tag{5}$$

Equation of State:

$$\rho = \rho_0\left[1 - \alpha_\vartheta\,(\vartheta - \vartheta_0) + \alpha_S\,(S - S_0)\right], \tag{6}$$

where $\mathbf{u}$ is the velocity, p is the pressure, $\mathbf{g}$ is acceleration due to gravity, ω is the angular velocity, I is the moment of inertia, S is concentration, C_v is specific heat, ρ_0 is density of fluid at temperature $\vartheta = \vartheta_0$, ρ is the density, α_S is the coefficient of concentration expansion, α_ϑ is the coefficient of thermal expansion, β is the micropolar heat conduction coefficient, χ is the thermal conductivity, γ is the shear kinematic viscosity, λ' and γ' are the bulk and shear spin-viscosity coefficients, ϑ is temperature, and ξ is the coupling viscosity coefficient or vortex viscosity. Without the presence of the vortex viscosity ξ, the bulk and shear spin viscosity λ', γ', micropolar heat conduction β, and concentration S, the equations (1)-(5) can be reduced to the classical problem of Newtonian fluids.

2.1 Steady state condition

When the fluid is motionless, the basic state of the quiescent fluid is indicated by:

$$\mathbf{u}_{bs} = 0, \quad \omega_{bs} = 0, \quad p = p_{bs}(z), \quad \rho = \rho_{bs}(z), \quad \frac{d\vartheta_{bs}}{dz} = -\frac{\Delta\vartheta h(z)}{d}, \quad \frac{dS_{bs}}{dz} = -\frac{\Delta S g(z)}{d}, \tag{7}$$

where the steady state denotes by the subscript "bs". ϑ_{bs} and S_{bs} are non-uniform at their origin in equation (7) while being heated or cooled at the boundary. Equation (7) now are substituted into equations (1)-(6), the equations governing the steady state are obtained as follows:

$$\frac{dp_{bs}}{dz} = -\rho_0 g, \quad \frac{d^2\vartheta_{bs}}{dz^2} = \frac{d^2 S_{bs}}{dz^2} = 0 \quad \text{and} \quad \rho_{bs} = \rho_0\Big[1 - \alpha_\vartheta(\vartheta_{bs} - \vartheta_0) + \alpha_S(S_{bs} - S_0)\Big]. \tag{8}$$

3 Linear Stability Analysis

Lets the fluid be perturbed in the steady state by infinitesimal thermal perturbation and their equation is given by:

$$\mathbf{u} = \mathbf{u}_{bs} + \mathbf{u}', \quad \rho = \rho_{bs} + \rho', \quad \vartheta = \vartheta_{bs} + \vartheta', \quad p = p_{bs} + p', \quad \omega = \omega_{bs} + \omega', \quad S = S_{bs} + S', \tag{9}$$

where the quantities of infinitesimal perturbations represent by prime. With the assumption that the principle of exchanges of stability is valid, therefore the current problems only take stationary convection into account. Now, substituted equation (9) into equations (1)–(6) together with the steady-state conditions (7), the linearising of the equations (1)-(6) are given in the form:

$$\nabla \cdot \mathbf{u}' = 0, \tag{10}$$

$$-\nabla p' - \rho' g\widehat{k} + (2\xi + \gamma)\,\nabla^2 \mathbf{u}' + \xi \nabla \times \omega' = 0, \tag{11}$$

$$(\lambda' + \gamma')\,\nabla\,(\nabla \cdot \omega') + \gamma' \nabla^2 \omega' + \xi\,(\nabla \times \mathbf{u}' - 2\omega') = 0, \tag{12}$$

$$w\frac{\Delta\vartheta}{d}h(z) + \chi\nabla^2\vartheta' + \frac{\beta}{\rho_0 C_v}\left[\nabla \times \omega' \cdot \left(-\frac{\Delta\vartheta}{d}h(z)\right)\widehat{k}\right], \tag{13}$$

$$\chi_s \nabla^2 S' - w\frac{\Delta S}{d}g(z) = 0, \tag{14}$$

$$\rho' = -\rho_0 \alpha_\vartheta \vartheta' - \rho_0 \alpha_S S'. \tag{15}$$

Equations (10)–(15) are then reduced to dimensionless equations using the definition of the following variables:

$$\begin{aligned} &(X^*, Y^*, Z^*) = \left(\frac{x}{d}, \frac{y}{d}, \frac{z}{d}\right), \quad \nabla^{*2} = d^2\nabla^2, \quad S^* = \frac{S'}{\Delta S}, \\ &\vartheta^* = \frac{\vartheta'}{\Delta\vartheta}, \quad w^* = \frac{w'}{\chi/d}, \quad \Omega^* = \frac{(\nabla \times \omega')}{\chi/d^3}, \quad \mathbf{u}^* = \frac{\mathbf{u}'}{\chi/d}. \end{aligned} \tag{16}$$

By substituting Equation (15) into Equation (11) and then performing curl operation twice on the resulting equation, also taking curl operation once on Equation (12) respectively. Using (16) on the resulting equations together with the equations (13) and (14), we have

$$Ra\nabla_1^2\vartheta - Rs\nabla_1^2 S + (1 + N_1)\nabla^4 w + N_1\nabla^2\Omega_Z = 0, \tag{17}$$

$$N_3\nabla^2\Omega_z - N_1\nabla^2 w - 2N_1\Omega_Z = 0, \tag{18}$$

$$\nabla^2\vartheta + h(Z)(w - N_5\Omega_Z) = 0, \tag{19}$$

$$\Gamma\nabla^2 S + wg(Z) = 0, \tag{20}$$

where

$$N_1 = \frac{\xi}{\xi + \gamma},$$

is coupling parameter $(0 \leq N_1 \leq 1)$, which represents the strength of the coupling between the rotation of fluid elements and the deformation of the fluid.

$$N_3 = \frac{\gamma'}{\xi + \gamma},$$

is couple stress parameter $(0 \leq N_3 \leq m)$, which explains the influence of internal rotational or couple stresses on the material's mechanical behavior.

$$N_5 = \frac{\beta}{\rho_0 C_v d^2},$$

is micropolar heat conduction parameter $(0 \leq N_5 \leq n)$, which represents the influence of microstructural characteristics, like internal rotations and the coupling between thermal and microrotation fields.

$$Ra = \frac{\rho_0 \alpha_\vartheta g \Delta \vartheta d^3}{(\xi + \gamma)\chi},$$

is Rayleigh number, which represents the ratio of the buoyancy force to the dissipative forces associated with heat transfer and

$$Rs = \frac{\rho_0 \alpha_S g \Delta S d^3}{(\xi + \gamma)\chi},$$

is a solutal Rayleigh number which explains the ratio of the buoyancy-driven force to the diffusive force associated with concentration gradients.

The asterisk have been dropped for simplicity and Ω_Z and w are the $Z-$component of $\vec{\omega}^*$ and $\vec{u}^*$.

The function $h(Z)$ and $g(Z)$ in the equations (19) and (20) are the non-uniform temperature gradient and concentration in more general form than the ones considered by [20] and [17]. The function of $h(Z)$ and $g(Z)$ are defined by (refer to: [8]),

$$h(Z) = a_{11}^* + 2a_{22}^*(Z-1) + 3 * a_{33}^*(Z-1)^2, \tag{21}$$
$$g(Z) = b_{11}^* + 2b_{22}^*(Z-1) + 3b_{33}^*(Z-1)^3, \tag{22}$$

where a_{11}^*, a_{22}^*, a_{33}^*, b_{11}^*, b_{22}^* and b_{33}^* are non-dimensional constant. The special cases $a_{11}^* = 1$, $a_{22}^* = 0$, $a_{33}^* = 0$ and $a_{11}^* = 0$, $a_{22}^* = -1$, $a_{33}^* = 0$ recover the linear and inverted parabolic basic state temperature distributions considered by [20]. Meanwhile, for $b_{11}^* = 1$, $b_{22}^* = 0$, $b_{33}^* = 0$ and $b_{11}^* = 0$, $b_{22}^* = -1$, $b_{33}^* = 0$ recover the linear and inverted parabolic basic state concentration distributions consider by [17] respectively.

Let the infinitesimal perturbation of w, Ω_Z, ϑ and S be taken to be periodic and which enables the normal modes solution to be taken in the form:

$$\big[w, \Omega_Z, \vartheta, S\big] = \big[W(Z), G_1(Z), \Theta(Z), S(Z)\big] e^{i(\kappa_x X + \kappa_y Y)}, \tag{23}$$

where $\kappa^2 = \left(\kappa_x^2 + \kappa_y^2\right)$ are wave number of disturbances in X- and Y- directions respectively. Substitute equation (23) into equations (17)–(20), we have

$$-Ra\Theta\kappa^2 + Rs\kappa^2 S + (1+N_1)(D^2-\kappa^2)^2 W + N_1(D^2-\kappa^2)G_1 = 0, \tag{24}$$
$$\Big[-N_3(D^2-\kappa^2) + 2N_1\Big]G_1 + N_1(D^2-\kappa^2)W = 0, \tag{25}$$
$$\Big[(D^2-\kappa^2)\Big]\Theta + (W - N_5 G_1)h(Z) = 0, \tag{26}$$
$$\Big[\Gamma(D^2-\kappa^2)\Big]S + W g(Z) = 0, \tag{27}$$

where $D = \dfrac{d}{dZ}$, subject to isothermal-permeable no-spin boundary condition as follows:

1. f-f:

$$W = D^2 W = G_1 = \Theta = S = 0, \tag{28}$$

at $Z = 0$ and $Z = 1$.

2. r-f:

$$W = DW = G_1 = \Theta = S = 0 \quad \text{and} \quad W = D^2W = G_1 = \Theta = S = 0, \tag{29}$$

at $Z = 0$ and $Z = 1$.

3. r-r:

$$W = DW = G_1 = \Theta = S = 0, \tag{30}$$

at $Z = 0$ and $Z = 1$.

Equations (24)–(27) were solved using the single-term Galerkin procedure, subject to the boundary conditions (28)–(30), by determining their eigenvalues. This method was chosen because it is developed around the idea of employing only local test and trial functions in the form of almost polynomials. The test and trial functions also span the entire domain and led to higher accuracy of outcomes. Instead of that, it is economics by staying away from certain matrix manipulation [7]. This approach also gives reasonable outcomes with the minimum of mathematics because the first approximation often gives the desired information [14, 6].

By taken the simplest solution for velocity, W and temperature, Θ in form of (refer to [11]):

$$[W, \Theta] = \Big[W_1(Z), \Theta_1(Z)\Big] \sin(\pi)Z,$$

subject to isothermal f-f boundary condition, with $N_1 = 0$, $N_3 = 0$ $N_5 = 0$, $h(Z) = 1$ and $S = 0$, equations (24)-(27) reduced to classical Rayleigh-Bénard problem for Newtonian fluids. Therefore we obtained the eigenvalue of Rayleigh number for Newtonian fluids as follows:

$$Ra = \frac{\left(\pi^2 + \kappa^2\right)^3}{\kappa^2}. \tag{31}$$

This result recovers the classical results obtained by [3] for cases of isothermal f-f boundary conditions.

In order to find the eigenvalue equation for the Rayleigh number of the Rayleigh-Bénard problem in double-diffusive micropolar fluids, first we multiply Equation (24) with W, Equation (25) with G_1, Equation (26) with Θ and Equation (27) with C respectively. The resulting equation then was integrated by parts with respect to $Z = 0$ and $Z = 1$. With the boundary conditions (28)–(30) and taking $W = AW_1$, $G_1 = BG_{11}$, $\Theta = E\Theta_1$ and $S = FS_1$ where A, B, E and F are constants and W_1, G_{11}, Θ_1, and S_1 are trial functions, the eigenvalue equation obtained is as follows:

$$Ra = -\left[\frac{\Big\langle \Theta_1\big(D^2 - \kappa^2\big)\Theta_1\Big\rangle\Big(h_9h_3h_7 - h_6h_4h_9 - h_3h_8^2\Big)}{a^2\Theta_1W_1h_3\Big(h_9h_1 - h_2h_8\Big)}\right], \tag{32}$$

where,

$$\begin{aligned}
h_1 &= \big\langle W_1\Theta_1h(Z)\big\rangle, & h_6 &= a^2Rs\big\langle W_1S_1\big\rangle,\\
h_2 &= -N_5\big\langle \Theta_1G_{11}h(Z)\big\rangle, & h_7 &= (1+N_1)\big\langle W_1(D^2-\kappa^2)^2W_1\big\rangle,\\
h_3 &= \Gamma\big\langle S_1(D^2-\kappa^2)S_1\big\rangle, & h_8 &= N_1\big\langle W_1(D^2-\kappa^2)G_{11}\big\rangle,\\
h_4 &= \big\langle W_1S_1g(Z)\big\rangle, & h_9 &= N_3\big\langle G_{11}(D^2-\kappa^2)G_{11}\big\rangle - 2N_1\big\langle G_{11}^2\big\rangle,\\
h_5 &= -a^2Ra\big\langle W_1\Theta_1\big\rangle,
\end{aligned}$$

where the integration represent by angle bracket $\langle\cdot\rangle$ is the integration with respect to Z from $Z = 0$ to $Z = 1$. A functional Euler-Lagrange equations for an extreme value of Ra is given by Equation (32). The Ra given in the equation (32) is a generalization of [17] for the cases of $h(Z) = 1$ for Linear, Parabola, and Inverted Parabola concentration functions. When $Rs = 0$ we recover results obtained by [8] for the cases Linear, Cubic 1, and Cubic 2 temperature gradient functions. The value of critical Rayleigh number Ra_c and critical wave number κ_c are obtained using

$$\frac{dRa}{d\kappa} = 0.$$

4 Results and Discussion

This study aims to examine the effect of cubic temperature gradient, cubic concentration gradient, and various micropolar parameters N_1, N_3 and N_5 on the onset of Rayleigh-Bénard convection in double-diffusive micropolar fluids. Table 1 presents the trial function for the different types of boundary conditions for both temperature and concentration.

Table 1: Trial function for different type of boundary conditions.

B.Cs	f-f	r-f	r-r
W_1	$Z - 2Z^3 + Z^4$	$3Z^2 - 5Z^3 + 2Z^4$	$Z^2 - 2Z^3 + Z^4$
Θ_1	$Z(Z-1)$	$Z(Z-1)$	$Z(Z-1)$
S_1	$Z(Z-1)$	$Z(Z-1)$	$Z(Z-1)$
G_{11}	$Z(Z-1)$	$Z(Z-1)$	$Z(Z-1)$

Table 2 gives the model of reference steady-state for temperature gradient and concentration gradient.

Table 2: Reference basic-state temperature and concentration gradient.

Model	Reference basic-state temperature gradient	$h(Z)$	a_{11}^*	a_{22}^*	a_{33}^*
	Reference basic-state concentration gradient	$g(Z)$	b_{11}^*	b_{22}^*	b_{33}^*
1	Linear		1	0	0
2	Cubic 1		0.34	0	0.66
3	Cubic 2		0	0	1

When $h(Z) = 1$, the results recovers [17]. Meanwhile, when $Rs = 0$, the results recover [8] for linear temperature and concentration gradient cases as shown in Table 3.

Table 3: Table of critical values of Rayleigh number and waves number for cases $Rs = 0$ with $h(Z) = 1$, $N_1 = 0.5$, $N_3 = 2$, $N_5 = 1$ and $\Gamma = 0.1$.

	Current Results		[8]	
B.Cs	Ra_c	κ_c	Ra_c	κ_c
f-f	1348.5704	2.2354	1348.5704	2.2354
r-f	2293.0478	2.6734	2293.0478	2.6738
r-r	3496.2213	3.1133	3496.2231	3.1133

In this paper, we will discuss how the value of the solutal Rayleigh number Rs will influence the value of the critical Rayleigh number, Ra_c. The graph of Ra_c versus Rs is plotted as Figures 2–4 for the three types of boundary conditions. Figure 2 represent the behavior of critical Rayleigh number versus solutal Rayleigh number for cases of linear temperature gradient and all concentration gradient model. Meanwhile Figure 3 and Figure 4 for the cases of Cubic 1 temperature gradient and Cubic 2 temperature gradient also for all concentration gradient models respectively. From all Figures, we can see that increasing the value of the solutal Rayleigh number Rs, decreases the critical value of critical Rayleigh number Ra_c for all models of temperature gradient consider in this study. Meaning that increasing the concentration gradient will influence the variation of density of the micropolar fluid, and the density becomes denser.

From Figures 2–4 also we discover that the critical Rayleigh number Ra_c, for cases of Cubic 2 temperature gradient together with Cubic 2 concentration gradient is most stable compared to Cubic 1 and Linear temperature gradient together with Cubic 1 and Linear concentration gradient. Out of the three boundaries considered in this study, we found that the r-r boundary is the most stable, followed by the r-f and f-f boundaries.

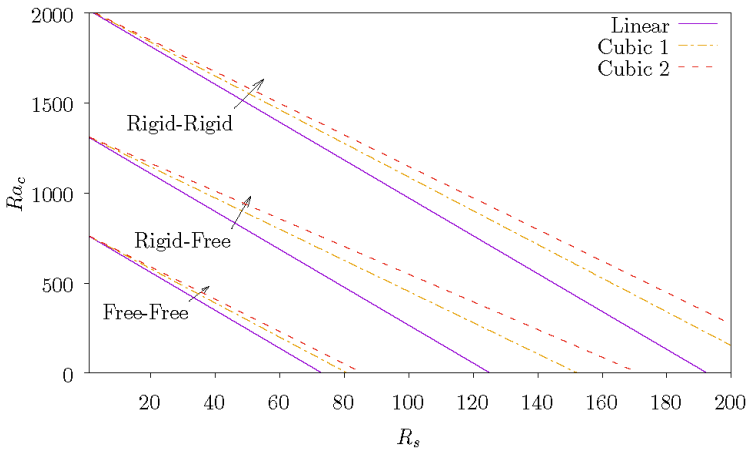

Figure 2: Rs vs Ra_c for cases of linear temperature gradient with $N_1 = 0.5$, $N_3 = 2$, $N_5 = 1$, $\Gamma = 0.1$ for Linear, Cubic 1 and Cubic 2 concentration gradient.

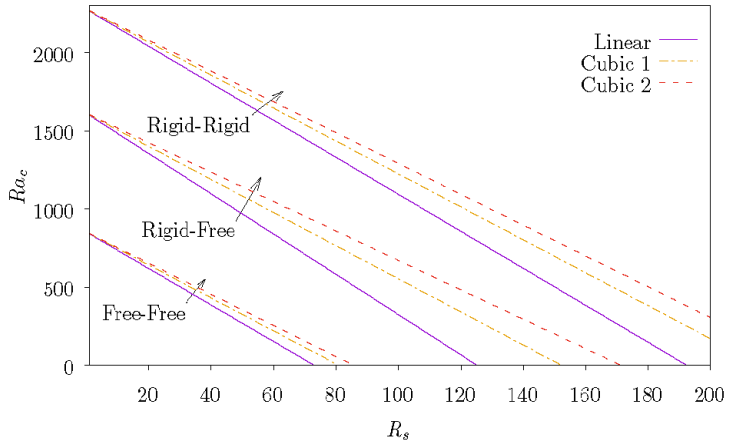

Figure 3: Rs vs Ra_c for cases of Cubic 1 temperature gradient with $N_1 = 0.5$, $N_3 = 2$, $N_5 = 1$, $\Gamma = 0.1$ for Linear, Cubic 1 and Cubic 2 concentration gradient.

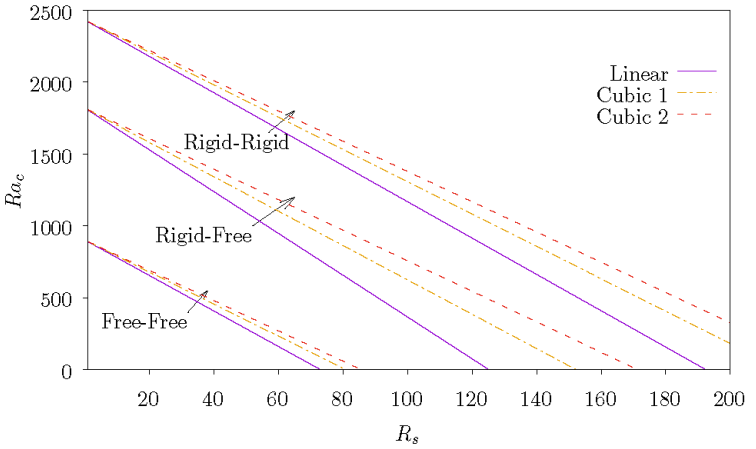

Figure 4: Rs vs Ra_c for cases of Cubic 2 temperature gradient with $N_1 = 0.5$, $N_3 = 2$, $N_5 = 1$, $\Gamma = 0.1$ for Linear, Cubic 1 and Cubic 2 concentration gradient.

Figures 5–7 represent the plots of critical Rayleigh number Ra_c versus coupling parameter N_1 for the cases of Linear (Figure 5), Cubic 1 (Figure 6) and Cubic 2 (Figure 7) temperature gradient with the different concentration gradient profiles together with r-r, r-f, and f-f boundary conditions respectively. From the figures, the results show that increasing the value of N_1 will increase the value of Ra_c for the Linear, Cubic 1, and Cubic 2 temperature gradient profile together with the Linear, Cubic 1, and Cubic 2 concentrations gradient profile. Increasing the values of N_1 indicates that the concentration between micro-elements also increases. The micro-elements generate a larger portion of the energy to develop gyrational velocity, hence delaying the process of convection and indirectly stabilizing the system. Out of the three temperature gradient profile, the results shows that the Cubic 2 temperature gradient together with the Cubic 2 concentration gradient are the most stable followed by the Cubic 1 and Linear temperature gradient together with Cubic 1 and Linear concentration gradient. Out of three boundaries, it is observed that r-r boundaries are the most stable compare to r-f and f-f boundaries as shown in Table 4.

Table 4: Table of critical values of Rayleigh number for cases $Rs = 25$ with $N_1 = 0.5$, $N_3 = 2$, $N_5 = 1$ and $\Gamma = 0.1$.

Temperature	Concentration	B.Cs		
$h(Z)$	$g(Z)$	f-f Ra_c	r-f Ra_c	r-r Ra_c
Linear	Linear	1012.280	1958.426	3163.852
	Cubic 1	1044.920	2017.886	3200.412
	Cubic 2	1061.734	2048.517	3219.247
Cubic 1	Linear	1122.281	22466.300	3575.691
	Cubic 1	1158.468	2541.176	3617.011
	Cubic 2	1177.110	2579.750	3638.297
Cubic 2	Linear	1188.832	2846.577	3832.703
	Cubic 1	1227.165	2933.000	3876.993
	Cubic 2	1246.912	2977.523	3899.808

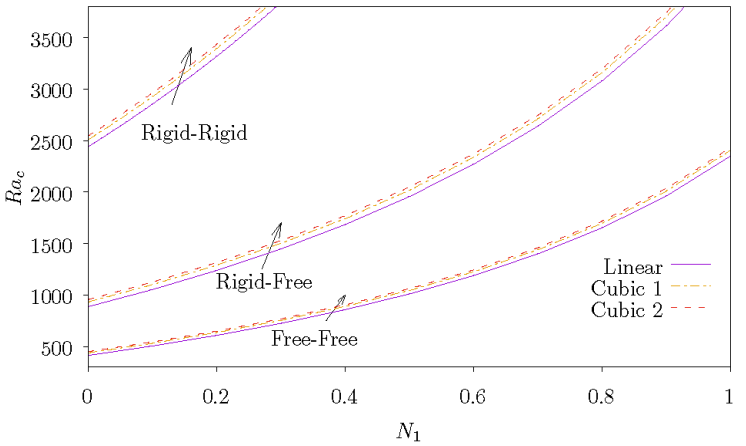

Figure 5: N_1 vs Ra_c for cases of linear temperature gradient with $Rs = 25$, $N_3 = 2$, $N_5 = 1$, $\Gamma = 0.1$ for Linear, Cubic 1 and Cubic 2 concentration gradient.

Plots of critical Rayleigh number Ra_c versus couple stress parameter N_3 for the different temperature gradient and concentration gradient profiles with a different type of boundary conditions shown as in Figure 8 for cases of Linear temperature gradient profile, Figure 9 for cases of Cubic 1 temperature gradient profile and Figure 10 for cases of Cubic 2 temperature gradient profile. From all plotted figures, it is obtained that the critical Rayleigh number Ra_c was decreased with increasing of N_3. The behavior of shear stress in the conservation of linear momentum was influenced by couple stress in angular momentum equations. This situation caused the micro-rotation of the fluid particle to decrease with increasing the couple stress of fluid. Therefore we can conclude that increasing the value of N_3 will destabilize the systems and these results are only valid for small values of N_3. Out of plotted Figures 8–10, the Cubic 2 temperature gradient and concentration gradient profile with r-r boundaries condition are the most stable compared with others.

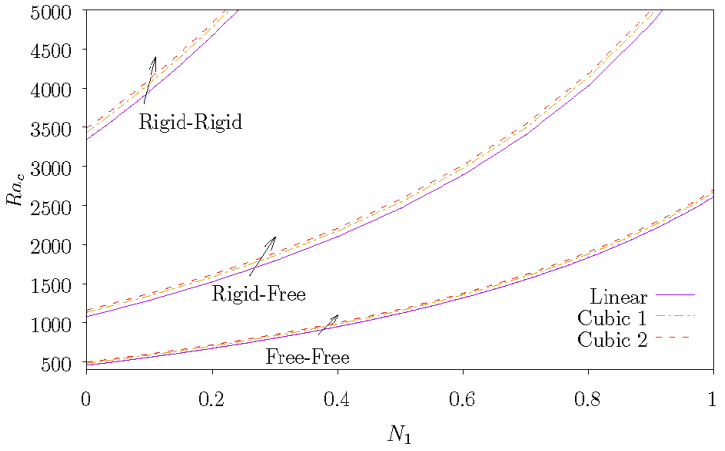

Figure 6: N_1 vs Ra_c for cases of Cubic 1 temperature gradient with $Rs = 25$, $N_3 = 2$, $N_5 = 1$, $\Gamma = 0.1$ for Linear, Cubic 1 and Cubic 2 concentration gradient.

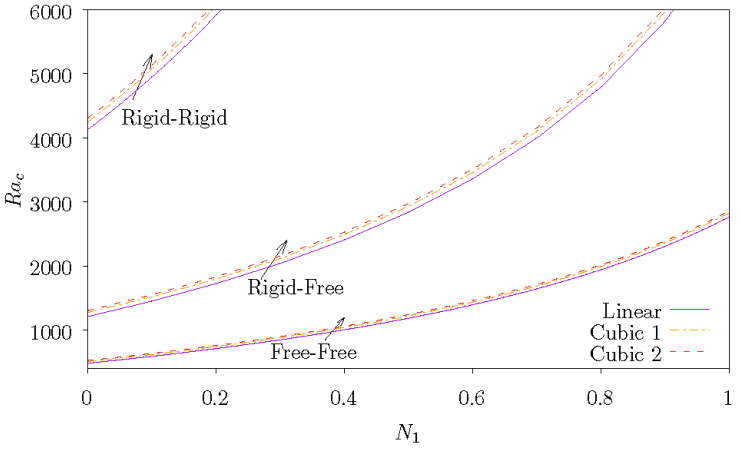

Figure 7: N_1 vs Ra_c for cases of Cubic 2 temperature gradient with $Rs = 25$, $N_3 = 2$, $N_5 = 1$, $\Gamma = 0.1$ for Linear, Cubic 1 and Cubic 2 concentration gradient.

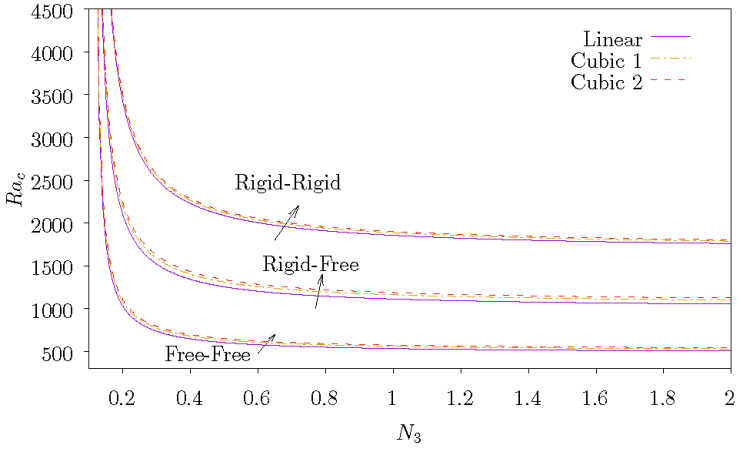

Figure 8: N_3 vs Ra_c for cases of linear temperature gradient with $Rs = 25$, $N_1 = 0.5$, $N_5 = 1$, $\Gamma = 0.1$ for Linear, Cubic 1 and Cubic 2 concentration gradient.

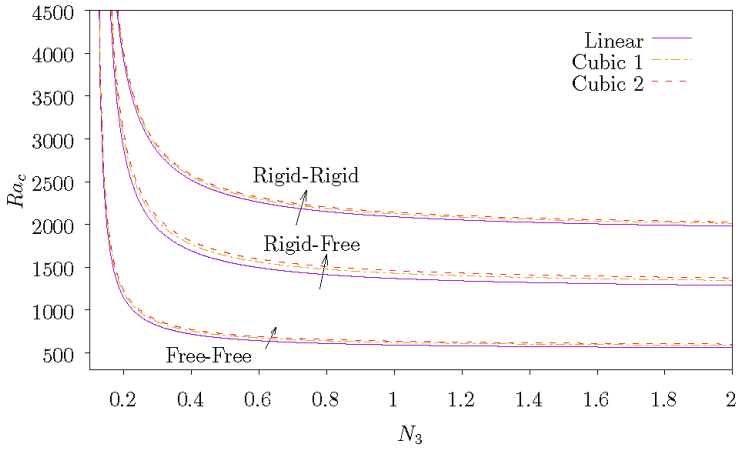

Figure 9: N_3 vs Ra_c for cases of Cubic 1 temperature gradient with $Rs = 25$, $N_1 = 0.5$, $N_5 = 1$, $\Gamma = 0.1$ for Linear, Cubic 1 and Cubic 2 concentration gradient.

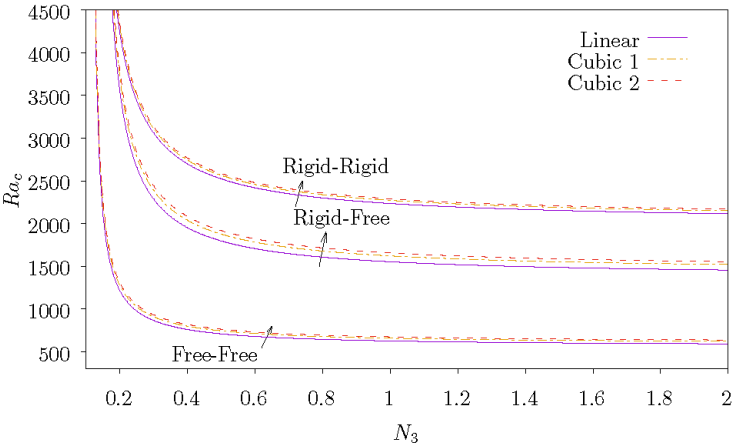

Figure 10: N_3 vs Ra_c for cases of Cubic 2 temperature gradient with $Rs = 25$, $N_1 = 0.5$, $N_5 = 1$, $\Gamma = 0.1$ for Linear, Cubic 1 and Cubic 2 concentration gradient.

The behavior of critical Rayleigh number Ra_c is also influenced by micropolar heat conduction parameter N_5, for the different types of temperature gradient and concentration gradient profiles with r-r, r-f, and f-f boundary conditions. This behavior was plotted as Figure 11 for the Linear temperature gradient profile, Figure 12 for the Cubic 1 temperature gradient profile, and Figure 13 for the Cubic 2 temperature gradient profile. Increasing the value of N_5 will increase the micro-elements of the fluid, this situation cause the heat transfer from bottom to top will reduce, therefore the density variation of the micropolar fluids becomes increased, hence increasing the value of Ra_c and this is true for all plotted figures. Therefore, we can conclude that reducing heat transfer will help the system be more stable by delaying the process of the onset of convection. Indirectly, N_5 will stabilize the systems. From Figures 11–13, it is observed that the Cubic 2 temperature gradient profile together with the Cubic 2 concentration gradient profile for cases of r-r boundary condition is most stable compared to others.

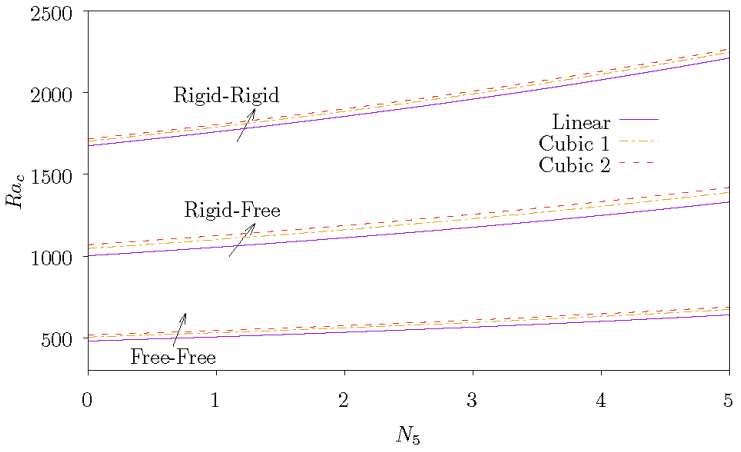

Figure 11: N_5 vs Ra_c for cases of linear temperature gradient with $Rs = 25$, $N_1 = 0.5$, $N_3 = 2$, $\Gamma = 0.1$ for Linear, Cubic 1 and Cubic 2 concentration gradient.

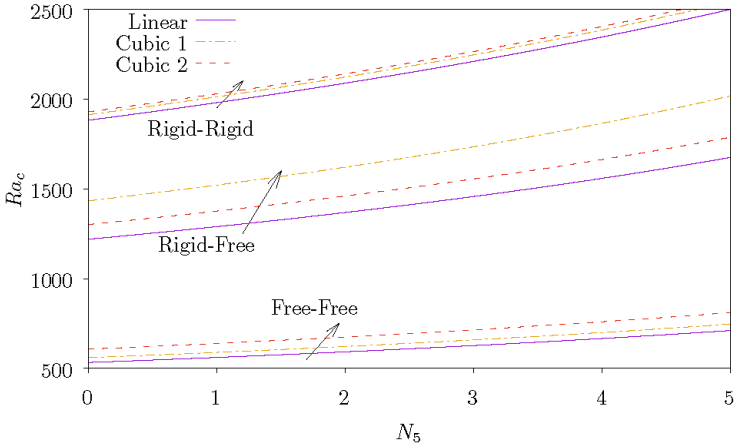

Figure 12: N_5 vs Ra_c for cases of Cubic 1 temperature gradient with $Rs = 25$, $N_1 = 0.5$, $N_3 = 2$, $\Gamma = 0.1$ for Linear, Cubic 1 and Cubic 2 concentration gradient.

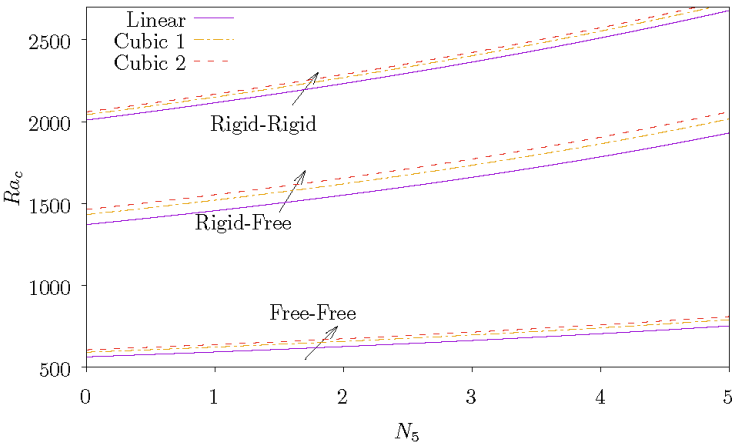

Figure 13: N_5 vs Ra_c for cases of Cubic 2 temperature gradient with $Rs = 25$, $N_1 = 0.5$, $N_3 = 2$, $\Gamma = 0.1$ for Linear, Cubic 1 and Cubic 2 concentration gradient.

For simplification, the effect of temperature and concentration gradient profile together with parameters N_1, N_3, N_5 and Rs to the investigated system can be summarized in Figure 14. From the block diagrams, we can see the control strategies consider in this research which are temperature and concentration gradient profiles that influenced parameters N_1 and N_5 put the systems in stable condition while for parameters N_3 and Rs put the systems in an unstable condition.

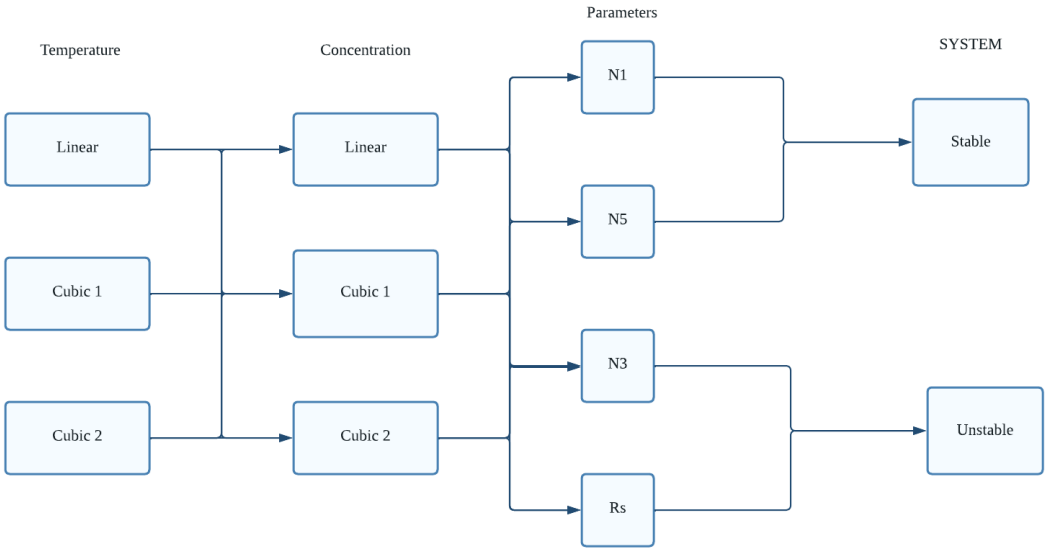

Figure 14: Control strategies diagram for the variety of temperature and concentration gradient profile and influenced parameters.

5 Conclusions

As mentioned in Section 1, the main objective of this study is to investigate the behavior of the onset of convection in double-diffusive micropolar fluids when both the cubic concentration gradient profile together with the cubic temperature profile were taken into account as a control mechanism for the onset of convection. Three different types of velocity boundary conditions which are r-r, r-f, and f-f were considered in this study. From the results obtained, it can be concluded that:

1. Out of three temperature gradient profiles together with three concentration profiles, we can conclude that the Cubic 2 profile is the most stable and holds the following inequality $Ra_{c1} < Ra_{c2} < Ra_{c3}$ respectively.
2. From the three boundary conditions consider in this study, we can conclude that $Ra_c^{f-f} < Ra_c^{r-f} < Ra_c^{r-r}$, where the velocity of boundary combinations represents by the superscripts.
3. The concentration force and buoyancy force reinforce each other by reducing the value of the critical Rayleigh number while raising the value of the solutal Rayleigh number.
4. The systems will become unstable due to the couple stress parameter N_3. Meanwhile, the system becomes stable due to the coupling parameter N_1 and micropolar heat conduction parameter N_5.
5. By selecting the proper non-uniform temperature and concentration gradient profiles, the onset of the Rayleigh-Bénard convection process is controllable.
6. By enclosing the micron-sized suspended particles, Rayleigh-Bénard convection in double-diffusive Newtonian fluids can be reduced.

Acknowledgement The authors would like to acknowledge Universiti Malaysia Terengganu for their financial support while doing this research.

Conflicts of Interest The authors declare no conflict of interest.

References

[1] S. Agarwal, B. S. Bhadauria, N. C. Sacheti, P. Chandran & A. K. Singh (2012). Non-linear convective transport in a binary nanofluid saturated porous layer. *Transport in Porous Media*, *93*(1), 29–49. https://doi.org/10.1007/s11242-012-9942-y.

[2] T. Ariman, M. A. Turk & N. D. Sylvester (1973). Microcontinuum fluid mechanics: A review. *International Journal of Engineering Science*, *11*(8), 905–930. https://doi.org/10.1016/0020-7225(73)90038-4.

[3] S. Chandrasekhar (1961). *Hydrodynamic and hyromagnetic stability*. Clarendon Press Melvin Stren, Oxford.

[4] A. C. Eringen (1964). Nonlinear theory of simple micro-elastic solids. *International Journal of Engineering Science*, *2*(2), 198–203. https://doi.org/10.1016/0020-7225(64)90004-7.

[5] A. C. Eringen (1966). Theory of micropolar fluids. *Journal of Mathematics and Mechanics*, *16*, 1–18.

[6] B. A. Finlayson (1972). *The method of weighted residuals and variational principles*. Academic Press, New York.

[7] C. A. J. Fletcher (1984). *Computational Galerkin Methods* (*Springer series in computational physics*). Springer-Verlag, Torronto.

[8] R. Idris (2011). *Analytical and numerical solution for linear and nonlinear stability of convection in fluid layer heated from below*. PhD thesis, Universiti Kebangsaan Malaysia, UKM Bangi, Selangor.

[9] I. K. Khalid, N. F. M. Mokhtar, Z. Siri, Z. B. Ibrahim & S. S. Abd. Gani (2019). Magneto-convection on the double-diffusive nanofuids layer subjected to internal heat generation in the presence of Soret and Dufour effects. *Malaysian Journal of Mathematical Sciences*, *13*(3), 397–418.

[10] I. K. Khalid, N. F. M. Mokhtar & Z. B. Ibrahim (2022). Control effect on Rayleigh-Bénard convection in rotating nanofluids layer with double-diffusive coefficients. *CFD Letters*, *14*(3), 79–95. https://doi.org/10.37934/cfdl.14.3.7995.

[11] G. Lebon & C. Perez-Garcia (1981). Convective instability of a micropolar fluid layer by the method of energy. *International Journal of Engineering Science*, *19*, 1321–1329. https://doi.org/10.1016/0020-7225(81)90015-X.

[12] G. Lukaszewicz (1999). *Micropolar Fluid Theory and Applications*. Birkhauser, Boston.

[13] N. F. M. Mokhtar, I. K. Khalid, Z. Siri, B. Ibrahim & S. A. Gani (2017). Control strategy on the double-diffusive convection in a nanofluid layer with internal heat generation. *Physics of Fluids*, *29*(10), 107105. https://doi.org/10.1063/1.4989584.

[14] D. A. Nield (1975). The onset of transient convective instability. *Journal of Fluid Mechanics*, *71*(3), 441–454. https://doi.org/10.1017/S0022112075002662.

[15] D. A. Nield & A. V. Kuznetsov (2010). The effect of vertical through flow on thermal instability in a porous medium layer saturated by nanofluid. *Transport in Porous Media*, *87*(3), 765–775. https://doi.org/10.1007/s11242-011-9717-x.

[16] D. A. Nield & A. V. Kuznetsov (2010). The onset of double-diffusive nanofluid convection in a layer of a saturated porous medium. *Transport in Porous Media*, *85*, 941–951. https://doi.org/10.1007/s11242-010-9600-1.

[17] S. Pranesh & A. K. Narayanappa (2012). Effect of non-uniform basic concentration gradient on the onset of double-diffusive convection in micropolar fluid. *Applied Mathematics*, *3*, 417–424.

[18] K. M. Prasad & P. R. Yasa (2021). Micropolar fluid flow in tapering stenosed arteries having permeable walls. *Malaysian Journal of Mathematical Sciences*, *15*(1), 147–160.

[19] T. Radko (2013). *Double-Diffusive Convection*. Cambridge University Press, Cambridge. https://doi.org/10.1017/CBO9781139034173.

[20] P. G. Siddheshwar & S. Pranesh (2002). Magnetoconvection in fluids with suspended particles under 1g and μg. *Aerospace Science and Technology*, *6*(2), 105–114. https://doi.org/10.1016/S1270-9638(01)01144-0.

[21] M. E. Stern (1960). The 'Salt-Fountain' and thermohaline convection. *Tellus*, *12*(2), 172–175. https://doi.org/10.3402/tellusa.v12i2.9378.

[22] H. Stommel, A. B. Arons & D. Blanchard (1956). An oceanographic curiosity: the perpetual salt fountain. *Deep Sea Research* (*1953*), *3*(2), 152—153. https://doi.org/10.1016/0146-6313(56)90095-8.